[Paleoceanography and Paleoclimatology]

Supporting Information for

Atmosphere-Ocean CO_2 Exchange Across the Last Deglaciation from the Boron Isotope Proxy

Jun Shao[1], Lowell D. Stott[1], William R. Gray[2, 3], Rosanna Greenop[2], Ingo Pecher[4], Helen L. Neil[5], Richard B. Coffin[6], and Bryan Davy[7] , James W.B. Rae[2]

[1] Department of Earth Science, University of Southern California, Los Angeles, USA

[2] School of Earth and Environmental Sciences, University of St Andrews, St Andrews, UK

[3] Laboratoire des Sciences du Climat et de l'Environnement (LSCE/IPSL), Gif-sur-Yvette, France

[4] School of Environment, University of Auckland, Auckland, New Zealand

[5] Department of Marine Geology, the National Institute of Water and Atmospheric Research, New Zealand

[6] Department of Physical and Environmental Sciences, Texas A&M University-Corpus Christi, USA

[7] Department of Marine Geosciences, GNS Science, New Zealand

Corresponding author: Jun Shao (junshao@usc.edu)

Contents of this file

Figures S1 to S10
Table S1 to S7

Additional Supporting Information (Files uploaded separately)

Captions for Figures S1 to S10

Captions for Tables S1 to S7

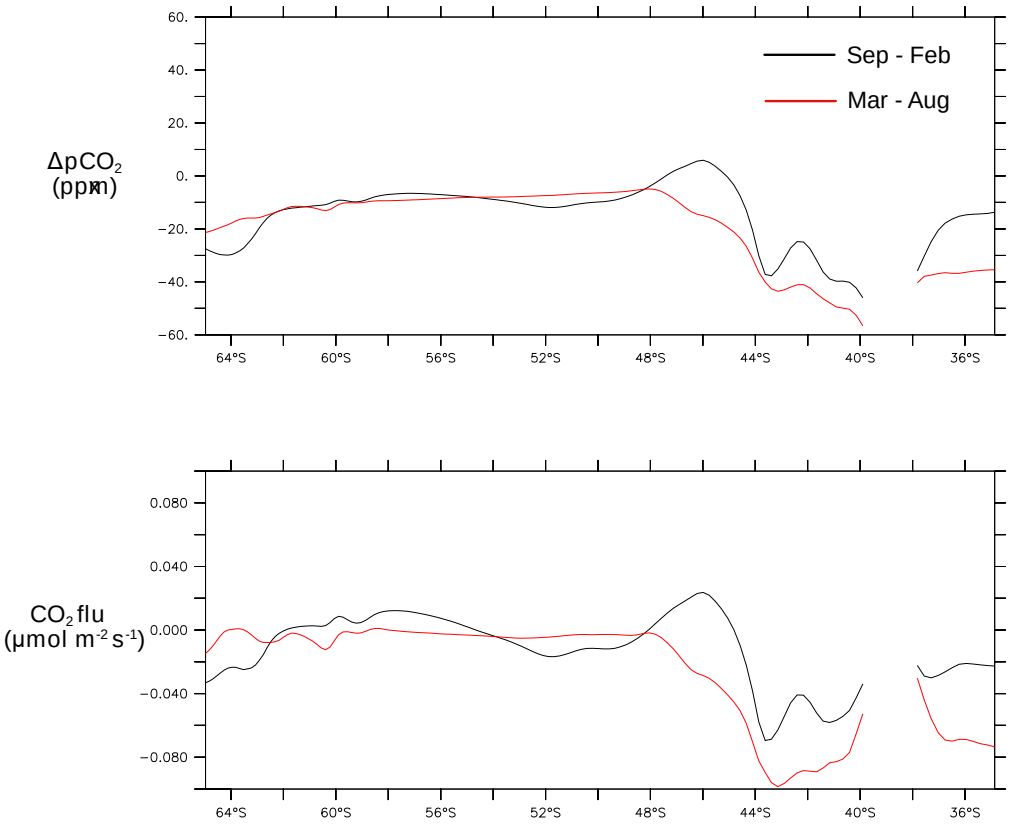

Figure S1. Meridional sections of ΔpCO_2 and CO_2 flux reanalysis data at at 177°E (year 2008-2012) from biogeochemical-sea ice-ocean state estimate (B-SOSE) as part of the SOCCOM

project (Verdy & Mazloff, 2017). The black (red) lines are 5-year 'climatology' of ΔpCO_2 and CO_2 flux between September to February (March to August).

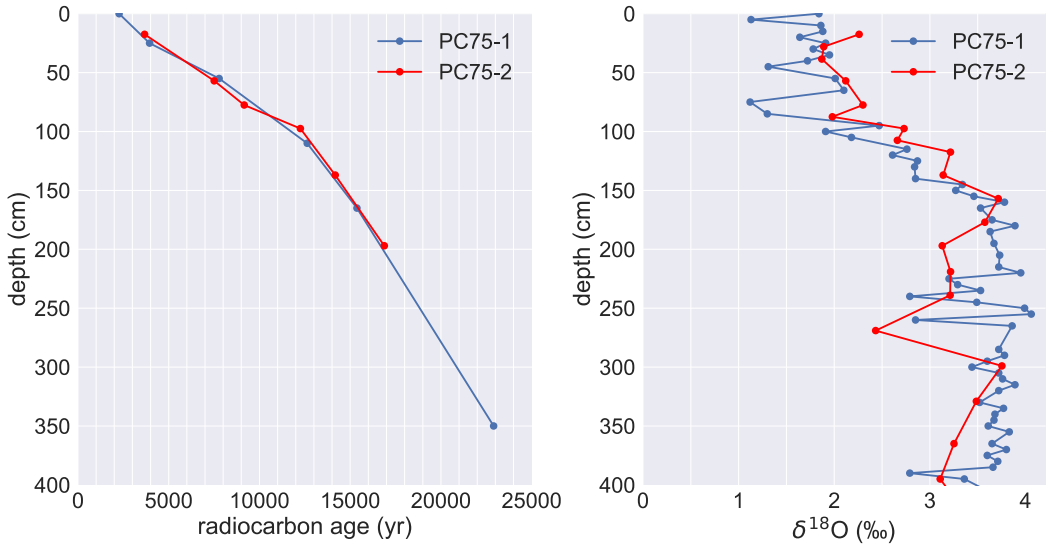

Figure S2: left panel: PC75-1 and PC75-2 raw planktic radiocarbon dates versus depth; right panel: PC75-1 and PC75-2 *G. inflata* oxygen isotope versus depth.

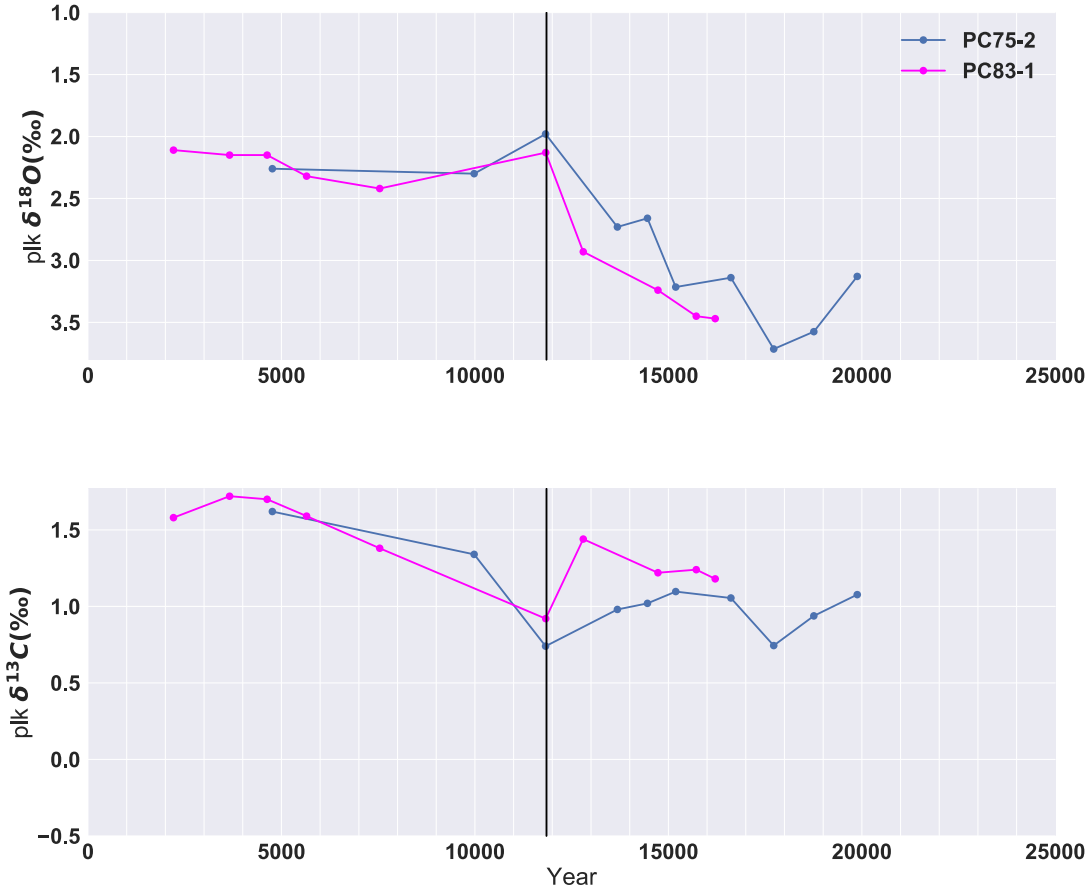

Figure S3: PC75-2 and PC83-1 *G. inflata* stable oxygen and carbon isotope. Based on the planktic stable isotope stratigraphy, we aligned the age of 88cm of PC83-1 to 88cm of PC75-2, the age of which is 11850 yrBP (the vertical black lines).

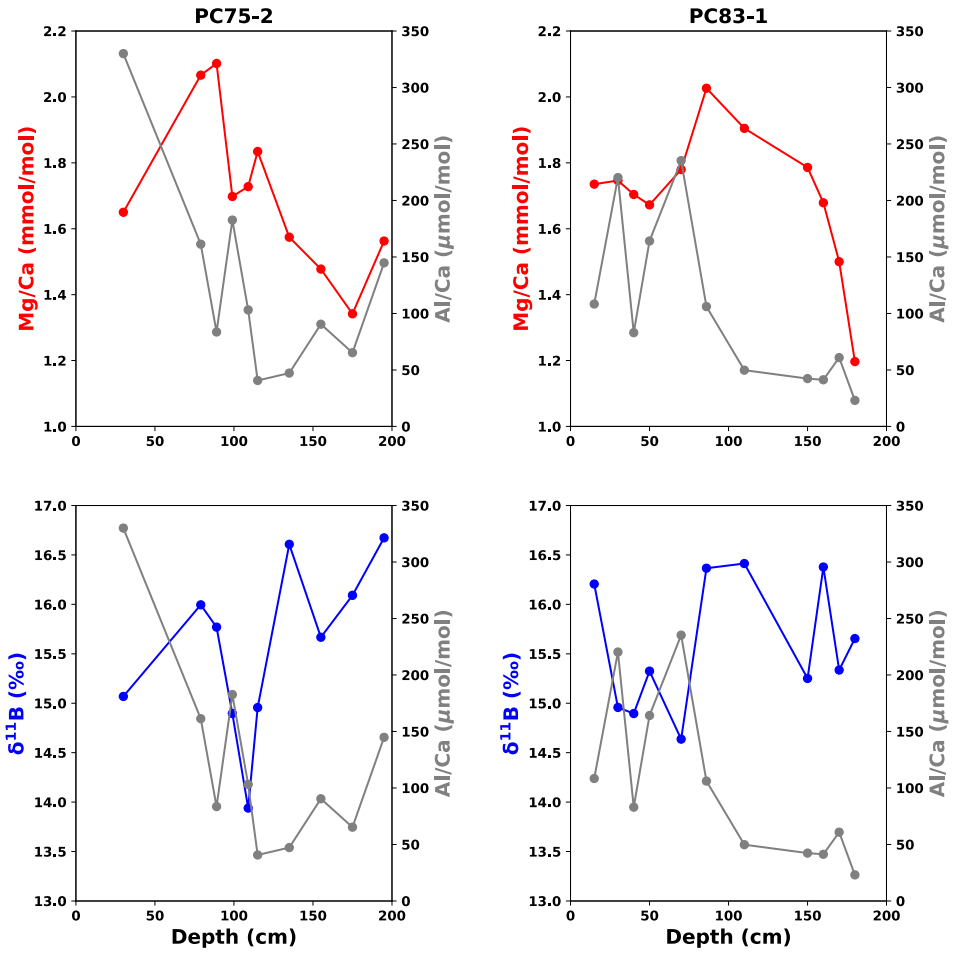

Figure S4. Mg/Ca and boron isotope data plotted with Al/Ca.

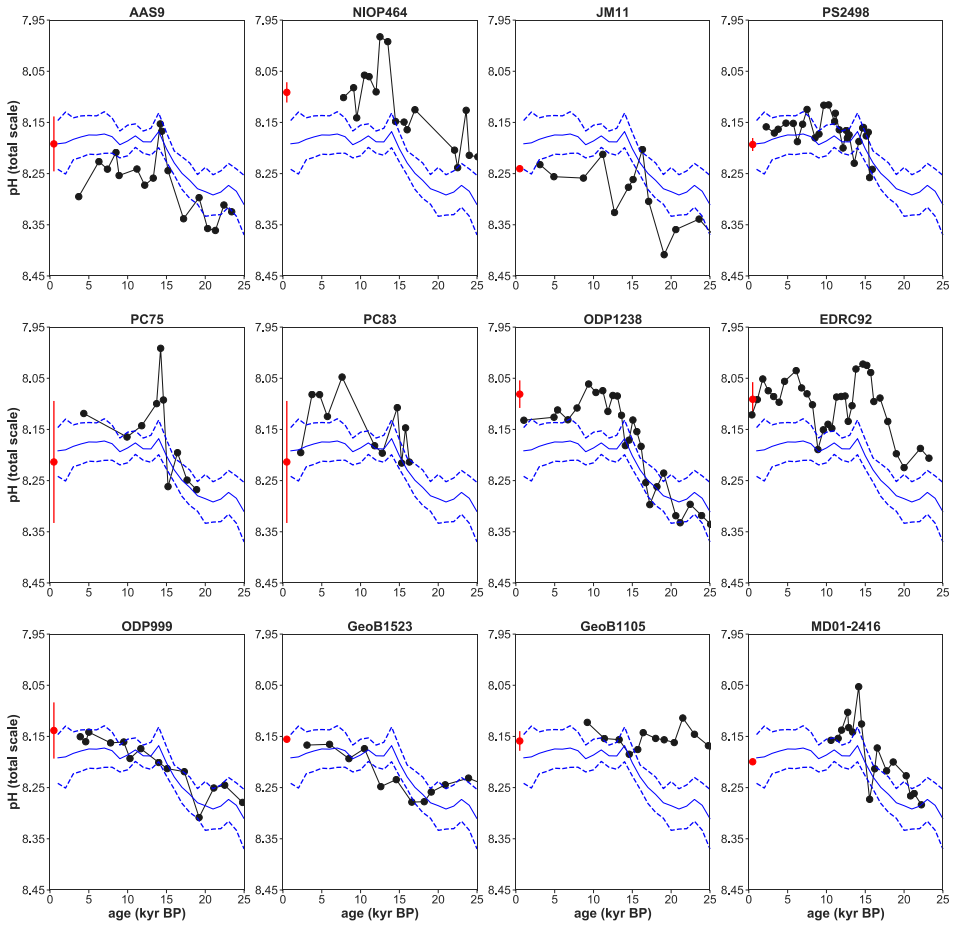

Figure S5. Individual uncorrected pH reconstructions (i.e. pH_{boron}) plotted against the composite pH built upon pH_{final}. The red dots represent pH_{site_preind} calculated from GLODAP V2 2016b (Lauvset et al., 2016).

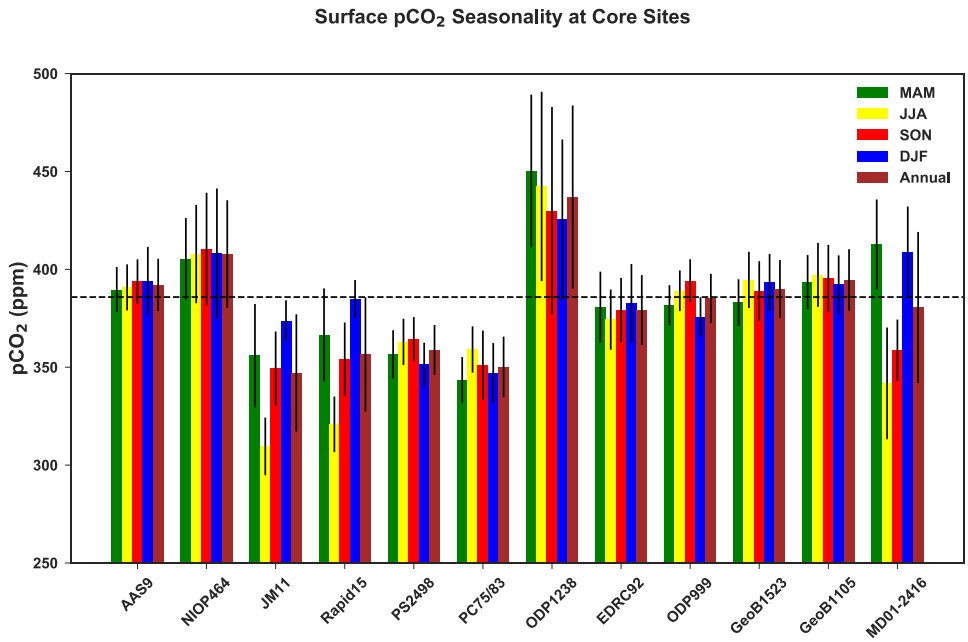

Figure S6. The climatology of seasonal and annual mean surface pCO_2 (year 2001-2015) (Landschützer et al., 2017) for each core site. The data is averaged over a 10° by 10° box around the core site. The black bars represent 1 standard error over the 15-year time period. Among these cores, JM11, Rapid 15 and MD01-2416 from high latitude oceans are characterized with strong seasonality. Rapid 15 is not included in our composite because it does not cover the LGM. For JM11, sediment trap data (Jonkers & Kučera, 2015) near the Norwegian Sea suggest that these is no *N. pachyderma* flux during winter, while for the rest of the year, the *N. pachyderma* flux is evenly distributed. Thus the geochemical signature of *N. pachyderma* would be an underestimate of the surface pCO_2. For MD01-2416, sediment trap data (Jonkers & Kučera, 2015) in the modern northwest Pacific display two abundance peaks during the spring (with high pCO_2) and autumn (with low pCO_2), the two seasonal fluxes are roughly equal and the average pCO_2 during the two seasons are close to the annual mean.

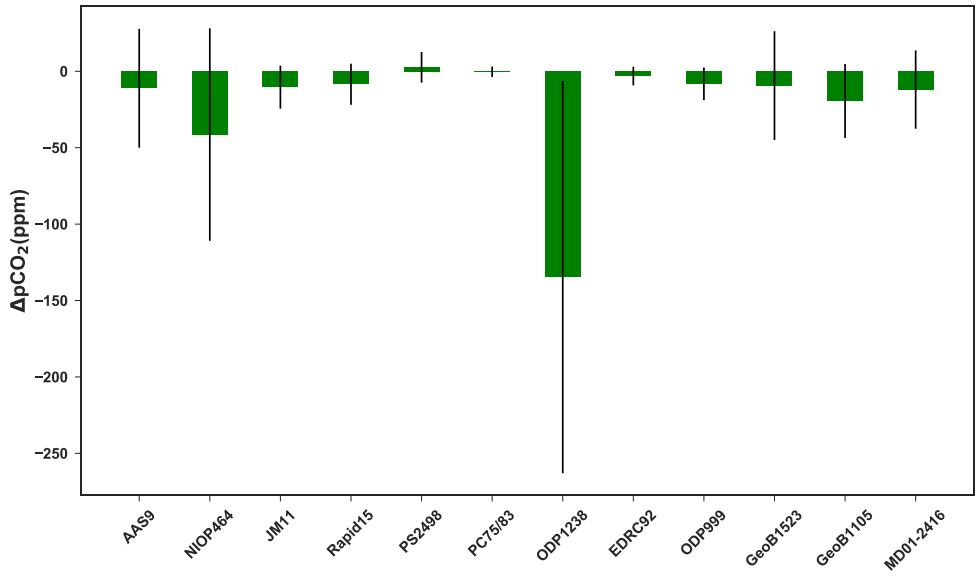

Figure S7. pCO_2 gradient between surface and the average of the first 50m at the core sites, the station data from GLODAP V2 (Olsen et al., 2016) is averaged over a 15°by 15°box around the core sites. For most of the cores in our composite, the depth difference is minimal (i.e. even though the foraminifera may not calcify not strictly at the surface, but the seawater carbonate chemistry state they record may still represent the surface condition). At the site of NIOP464, the surface-subsurface difference is up to 50 ppm on average, however the station data were all taken in a single cruise in Aug 1995, thus it is not clear of those station data are truly representative to the long term condition. The site of ODP1238 is affected by El-Niño, the station data were taken between year 1992-1994 when El-Niño was in the positive phase (i.e. the eastern equatorial Pacific is more stratified). Thus the 100~150 ppm of surface-subsurface ΔpCO_2 should be taken as a maximum.

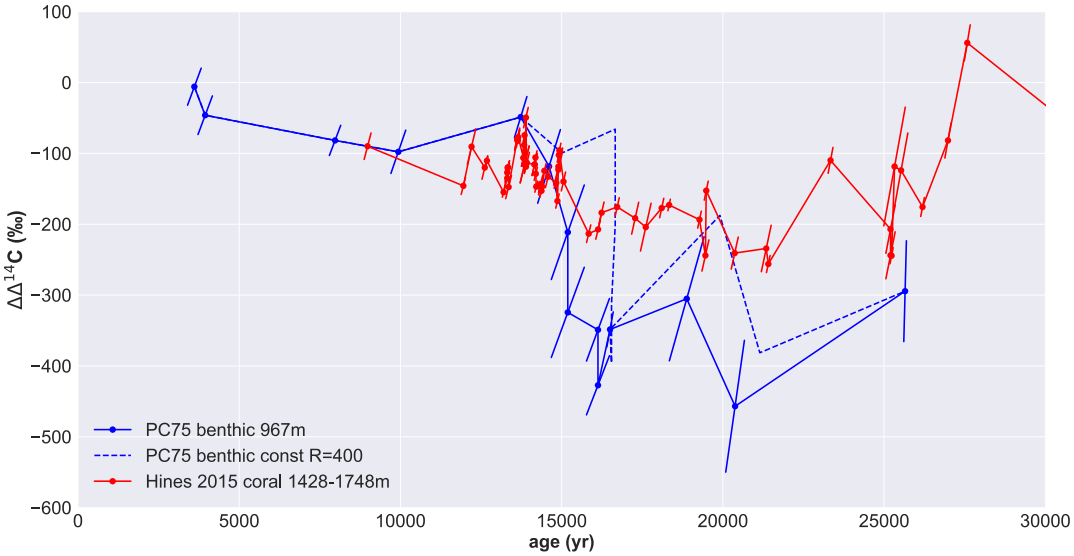

Figure S8. PC75 benthic - atmospheric $\Delta^{14}C$ offset ($\Delta\Delta^{14}C$) and Tasman Sea coral (43°S-47°S 144°E-152°E) – atmospheric $\Delta\Delta^{14}C$ (Hines et al., 2015). The dotted blue line assumes a constant reservoir age (~ 400 yrs) over the entire PC75 record.

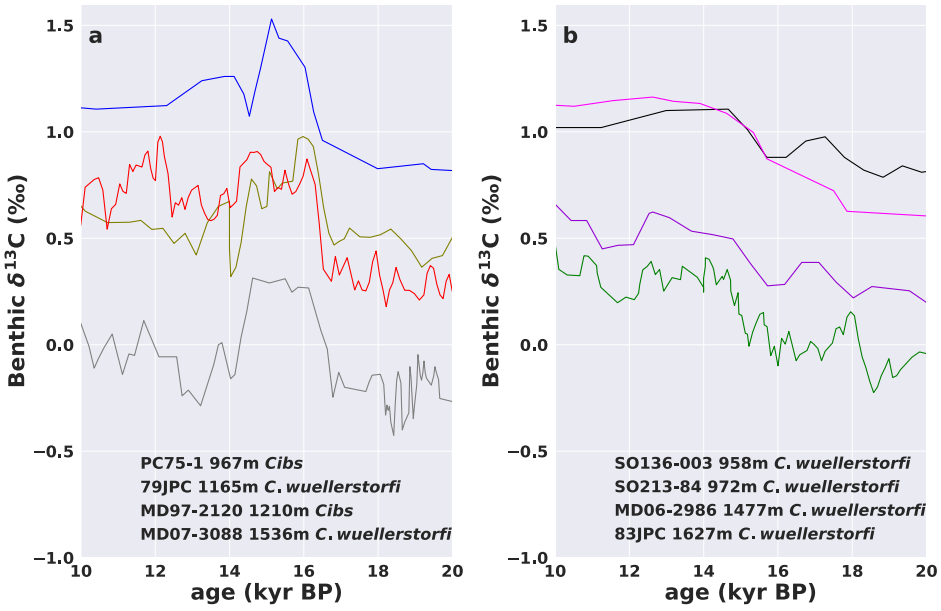

Figure S9, panel a: benthic $\delta^{13}C$ records from the South Pacific that show first rapid increase and then decline between 16.5-14 kyrBP (this study; Pahnke & Zahn, 2005; Rose et al., 2010; Siani et al., 2013). Panel b: benthic $\delta^{13}C$ records from the South Pacific that show a general increase between 16.5-14 kyrBP (Ronge et al., 2015; Sikes et al., 2016). The lines are 3-point running average.

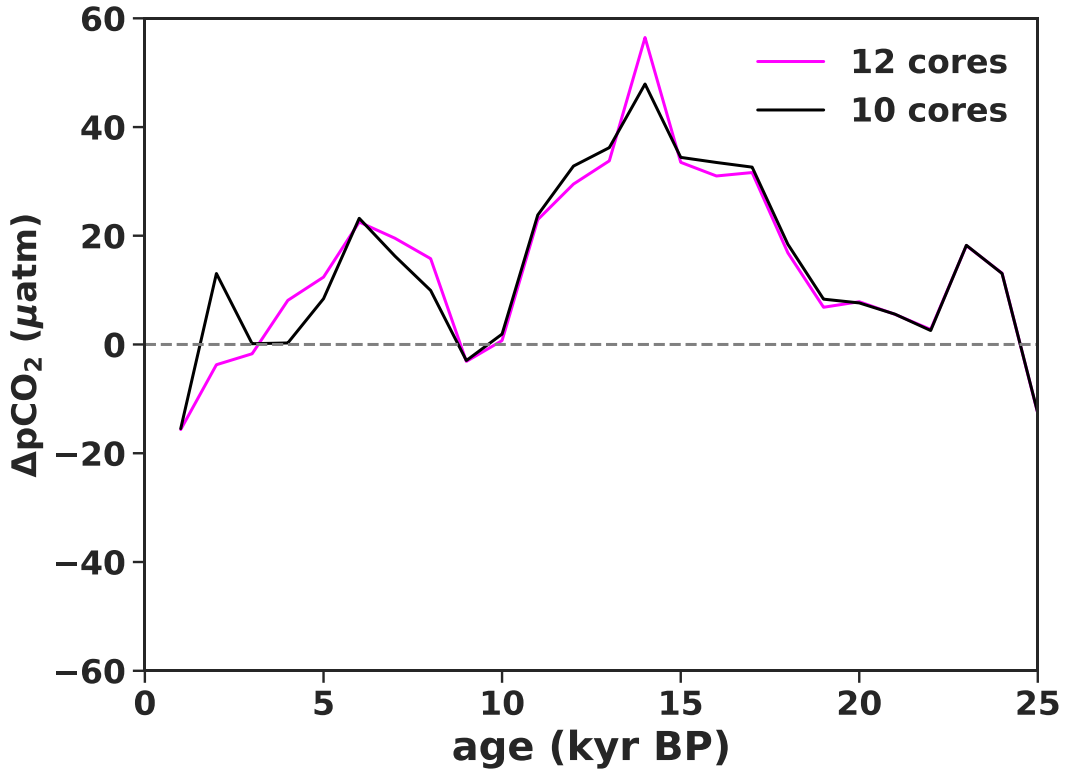

Figure S10, ΔpCO_2 composite with all 12 cores included (magenta), and with PC75-1 and PC83-2 from this study excluded (black).

core name	mid-depth(cm)	^{14}C ages (yr BP)	^{14}C age error	Species	Accession Number
PC75-1	0	2267	20	mixed planktics	NZA58474/R40687-1
PC75-1	25	3947	29	mixed planktics	NZA58940/R40701-1
PC75-1	25	4005	54	mixed benthics	NZA58503/R40687-3
PC75-1	55	7776	31	mixed planktics	NZA58475/R40687-4
PC75-1	110	12630	59	mixed planktics	NZA58941/R40701-2

PC75-1	165	15371	319	mixed planktics	NZA58504/R40687-6
PC75-1	165	16102	176	mixed benthics	NZA58929/R40693-1
PC75-1	230	19955	708	mixed benthics	NZA58505/R40687-7
PC75-1	350	22904	1221	mixed planktics	NZA58507/R40687-9
PC75-1	350	22959	446	mixed benthics	NZA58931/R40693-3
PC75-2	17.5	3670	20	*G. inflata*	UCIAMS-189011
PC75-2	17.5	3414	20	mixed benthics	UCIAMS-189012
PC75-2	57	7505	25	*G. inflata*	UCIAMS-189013
PC75-2	57	7800	25	mixed benthics	UCIAMS-189014
PC75-2	77.5	9160	40	*G. inflata*	UCIAMS-189016
PC75-2	77.5	9630	100	mixed benthics	UCIAMS-189015
PC75-2	97.5	12255	50	*G. inflata*	UCIAMS-189017
PC75-2	97.5	12200	70	mixed benthics	UCIAMS-189018
PC75-2	117.5	13240	140	mixed benthics	UCIAMS-189021
PC75-2	137	14175	45	*G. inflata*	UCIAMS-189022
PC75-2	137	15090	190	mixed benthics	UCIAMS-189023
PC75-2	137	14195	45	mixed benthics	UCIAMS-189024
PC75-2	157	16520	140	mixed benthics	UCIAMS-189017
PC75-2	157	15850	110	mixed benthics	UCIAMS-189026
PC75-2	197	16880	250	*G. bulloides*	UCIAMS-190039
PC75-2	197	17610	370	mixed benthics	UCIAMS-190040
PC83-1	13	2610	25	*G. inflata*	UCIAMS-189028
PC83-1	68	7135	25	*G. inflata*	UCIAMS-189029
PC83-1	178.5	14790	170	*G. inflata*	UCIAMS-189030

Table S1. Planktic and benthic radiocarbon dates

core name	mid-depth(cm)	$\delta^{18}O$(‰)	$\delta^{13}C$(‰)
PC75-1	0	1.84	1.05
PC75-1	5	1.13	1.22
PC75-1	10	1.86	1.3
PC75-1	15	1.88	1.47
PC75-1	20	1.64	1.41
PC75-1	25	1.91	1.45
PC75-1	30	1.78	1.31
PC75-1	35	1.95	1.19
PC75-1	40	1.72	1.32
PC75-1	45	1.31	1.41
PC75-1	55	2.01	1.36
PC75-1	65	2.1	1.17
PC75-1	75	1.12	0.83
PC75-1	85	1.3	0.5
PC75-1	95	2.47	0.98
PC75-1	100	1.91	0.63
PC75-1	105	2.18	-0.01
PC75-1	115	2.76	0.81
PC75-1	120	2.61	0.7
PC75-1	125	2.87	0.71
PC75-1	130	2.84	0.89
PC75-1	140	2.85	0.38
PC75-1	145	3.34	0.76
PC75-1	150	3.27	1.01
PC75-1	155	3.46	0.59
PC75-1	160	3.78	0.54
PC75-1	165	3.53	1.17
PC75-1	175	3.65	0.33
PC75-1	180	3.89	1.08
PC75-1	185	3.63	0.93
PC75-1	195	3.67	0.54
PC75-1	205	3.73	0.7
PC75-1	215	3.72	0.82
PC75-1	220	3.95	0.91
PC75-1	225	3.2	0.17
PC75-1	230	3.29	0.11
PC75-1	235	3.53	0.28
PC75-1	240	2.79	0.89
PC75-1	245	3.49	0.82

PC75-1	250	3.99	0.72
PC75-1	255	4.06	1.07
PC75-1	260	2.85	0.57
PC75-1	265	3.86	0.62
PC75-1	285	3.72	0.74
PC75-1	290	3.78	0.67
PC75-1	295	3.6	0.82
PC75-1	300	3.44	1.09
PC75-1	305	3.72	0.67
PC75-1	310	3.76	0.3
PC75-1	315	3.89	0.97
PC75-1	320	3.72	0.04
PC75-1	330	3.52	0.54
PC75-1	335	3.77	0.63
PC75-1	340	3.68	0.95
PC75-1	345	3.67	0.71
PC75-1	350	3.61	1.17
PC75-1	355	3.83	0.82
PC75-1	365	3.65	0.24
PC75-1	370	3.8	0.63
PC75-1	375	3.6	0.56
PC75-1	380	3.71	0.73
PC75-1	385	3.66	0.27
PC75-1	390	2.79	0.18
PC75-1	395	3.36	0.43
PC75-1	405	3.6	0.5
PC75-2	17.5	2.26	1.573
PC75-2	28	1.89	1.62
PC75-2	38.5	1.87	1.31
PC75-2	57	2.12	1.5
PC75-2	77.5	2.3	1.34
PC75-2	87.5	1.98	0.74
PC75-2	97.5	2.73	0.98
PC75-2	107.5	2.66	1.02
PC75-2	117.5	3.215	1.097
PC75-2	137	3.139	1.055
PC75-2	157	3.715	0.744
PC75-2	177	3.575	0.938
PC75-2	197	3.129	1.077
PC75-2	219	3.22	1.14
PC75-2	239	3.21	0.99
PC75-2	269	2.43	1.33
PC75-2	299	3.75	0.75

PC75-2	329	3.49	0.84
PC75-2	365	3.25	1.10
PC75-2	395	3.11	1.12
PC83-1	13	2.11	1.58
PC83-1	28	2.15	1.72
PC83-1	38	2.15	1.7
PC83-1	48.5	2.32	1.59
PC83-1	68	2.42	1.38
PC83-1	88	2.13	0.92
PC83-1	108	2.93	1.44
PC83-1	148	3.24	1.22
PC83-1	168.5	3.45	1.24
PC83-1	178.5	3.47	1.18

Table S2. *G.inflata* oxygen and carbon stable isotope results.

core name	mid-depth(cm)	$\delta^{18}O$(‰)	$\delta^{13}C$(‰)
PC75-1	0	2.08	1.02
PC75-1	15	2.1	1.28
PC75-1	20	2.05	1.19
PC75-1	25	2.15	1.4
PC75-1	30	2.13	1.51
PC75-1	35	2.16	1.36
PC75-1	40	2.14	1.55
PC75-1	45	2.12	1.43
PC75-1	50	2	1.38
PC75-1	55	2.22	1.22
PC75-1	60	2.22	1.21
PC75-1	65	2.21	1.19
PC75-1	70	2.13	1.19
PC75-1	75	2.22	1.14
PC75-1	80	2.51	1.02
PC75-1	90	2.11	1.16
PC75-1	95	2.52	1.19
PC75-1	100	2.66	1.37
PC75-1	105	3.05	1.22
PC75-1	110	3.01	1.19
PC75-1	115	2.85	1.12
PC75-1	120	2.8	0.91
PC75-1	125	2.99	1.54
PC75-1	135	3.36	1.44
PC75-1	140	3.65	1.61
PC75-1	145	3.62	1.27
PC75-1	155	3.8	1.4
PC75-1	160	3.91	1.24
PC75-1	165	4.08	0.64
PC75-1	185	4.11	1
PC75-1	205	3.94	0.84
PC75-1	210	4.1	0.71
PC75-1	235	3.78	0.92
PC75-1	255	3.86	0.81
PC75-1	265	3.94	0.81
PC75-1	270	3.86	0.63
PC75-1	285	3.82	0.69
PC75-1	290	3.92	0.55
PC75-1	295	3.68	1.07
PC75-1	310	3.97	0.54
PC75-1	315	3.67	1.15
PC75-1	320	3.68	0.69

PC75-1	345	3.69	1.11
PC75-1	355	3.61	1.01

Table S3. *Cibicides* oxygen and carbon stable isotope results.

core name	mid-depth(cm)	dR (yr)	dR error (1SE)	calibrated age (yr)	calibrated age error (1SE)
PC75-1	0	0	100	1894	199
PC75-1	25	0	100	3945	224
PC75-1	55	0	100	7973	172
PC75-1	110	0	100	14385	322
PC75-2	17.5	0	100	3609	213
PC75-2	57	0	100	8283	176
PC75-2	77.5	0	100	9935	230
PC75-2	97.5	0	100	13729	195
PC75-2	137	900	200	15190	540
PC75-2	197	900	200	18879	540
PC83-1	13	0	100	2299	209
PC83-1	68	0	100	7621	159
PC83-1	178.5	900	200	16280	555

Table S4. Reservoir ages and calibrated ages.

Core name	Age (kyr BP)	$\delta^{11}B$ (‰)	$\delta^{11}B$ 2SD (‰)	Mg/Ca (mmol/mol)	pH (total scale)	pCO_2 (µatm)	Al/Ca (µmol/mol)
PC75-2	3.61	15.0	0.6	1.71	8.12	319.1	330.0
PC75-2	9.92	16	0.27	2.07	8.17	288.6	161.3
PC75-2	11.81	15.7	0.28	2.10	8.14	304.6	83.6
PC75-2	13.73	14.9	0.26	1.70	8.10	334.0	182.7
PC75-2	14.25	13.9	0.29	1.73	7.99	431.6	103.1
PC75-2	14.61	14.9	0.29	1.83	8.09	341.2	40.7
PC75-2	15.2	16.6	0.25	1.57	8.26	223.1	47.2
PC75-2	16.42	15.6	0.5	1.48	8.20	262.7	90.5
PC75-2	17.65	16.0	0.41	1.34	8.25	228.9	65.3
PC75-2	18.88	16.6	0.34	1.56	8.27	219.5	144.8
PC83-1	2.29	16.2	0.27	1.74	8.20	266.9	108.4
PC83-1	3.75	14.9	0.35	1.75	8.08	358.2	220.3
PC83-1	4.72	14.9	0.3	1.7	8.08	358.5	83.0
PC83-1	5.73	15.3	0.51	1.67	8.13	320.7	164.1
PC83-1	7.62	14.6	0.25	1.78	8.05	392.3	235.3
PC83-1	11.81	16.3	0.26	2.03	8.18	276.4	106.1
PC83-1	12.8	16.4	0.34	1.9	8.20	265.6	49.8
PC83-1	14.73	15.2	0.38	1.79	8.11	335.0	42.4
PC83-1	15.29	16.3	0.27	1.68	8.22	251.8	41.3
PC83-1	15.79	15.3	0.24	1.5	8.15	300.6	60.9
PC83-1	16.28	15.6	0.31	1.2	8.21	250.9	23.0

Table S5. PC75-2 and PC83-1 boron isotope, trace element data, calculated pH_{boron} and pCO_{2boron}

Age (kyr BP)	pH (total scale)	pH error (2SE)	pCO_2 (µatm)	ΔpCO_2 (µatm)	ΔpCO_2 error (2SE)
1	8.192	0.047	262.35	-15.65	60.66
2	8.190	0.058	271.76	-3.73	64.64
3	8.183	0.042	272.48	-1.71	40.75
4	8.178	0.045	277.28	8.10	42.46
5	8.174	0.037	279.08	12.39	44.79
6	8.175	0.038	280.41	22.53	52.55
7	8.173	0.044	280.14	19.55	57.56
8	8.178	0.037	276.06	15.77	47.85
9	8.194	0.027	261.08	-3.11	29.27
10	8.186	0.032	267.39	0.73	36.59
11	8.176	0.025	275.58	22.97	38.82
12	8.188	0.022	268.80	29.50	42.27
13	8.188	0.027	269.83	33.77	50.16
14	8.168	0.036	284.48	56.45	67.26
15	8.202	0.032	257.78	33.50	49.76
16	8.229	0.024	235.20	31.00	42.53
17	8.249	0.032	220.30	31.63	50.32
18	8.263	0.033	209.50	16.86	45.94
19	8.280	0.029	200.90	6.86	31.94
20	8.284	0.048	197.87	7.85	51.87
21	8.292	0.038	194.27	5.56	43.05
22	8.286	0.043	192.50	2.76	47.44
23	8.273	0.043	202.27	18.18	55.70
24	8.285	0.044	193.76	13.10	55.99
25	8.310	0.054	171.97	-12.69	51.69

Table S6. 12-core composite pH, pCO_2 and ΔpCO_2 data

Core name	mid-depth (cm)	cal age (yr)	cal age error 1SE (yr)	$\Delta^{14}C$ (‰)	$\Delta^{14}C$ error (‰)
PC75-1	25	3945	224	-21	27
PC75-1	165	16500	100	-8	25
PC75-1	230	20378	290	-19	93
PC75-1	350	25650	40	277	71
PC75-2	17.5	3609	213	12	26
PC75-2	57	7973	176	-6	21
PC75-2	77.5	9935	230	3	31
PC75-2	97.5	13729	195	153	29
PC75-2	117.5	14609	353	126	52
PC75-2	137	15190	512	-40	64
PC75-2	137	15190	512	73	67
PC75-2	157	16126	356	-100	42
PC75-2	157	16126	356	-22	44
PC75-2	197	18879	540	96	88

Table S7. PC75 benthic $\Delta^{14}C$ results

Supplement Reference:

Hines, S. K. V., Southon, J. R., & Adkins, J. F. (2015). A high-resolution record of Southern Ocean intermediate water radiocarbon over the past 30,000 years. *Earth and Planetary Science Letters*, *432*, 46–58. https://doi.org/10.1016/j.epsl.2015.09.038

Jonkers, L., & Kučera, M. (2015). Global analysis of seasonality in the shell flux of extant planktonic Foraminifera. *Biogeosciences*, *12*(7), 2207–2226. https://doi.org/10.5194/bg-12-2207-2015

Landschützer, P., N. Gruber and D.C.E. Bakker (2017). An updated observation-based global monthly gridded sea surface pCO2 and air-sea CO2 flux product from 1982 through 2015 and its monthly climatology (NCEI Accession 0160558). Version 2.2. NOAA National Centers for Environmental Information. Dataset. [2017-07-11]

Lauvset, S. K., Key, R. M., Olsen, A., van Heuven, S., Velo, A., Lin, X., et al. (2016). A new global interior ocean mapped climatology: the 1◦ × 1◦ GLODAP version 2, 16.

Olsen, A., Key, R. M., Van Heuven, S., Lauvset, S. K., Velo, A., Lin, X., et al. (2016). The global ocean data analysis project version 2 (GLODAPv2) - An internally consistent data product for the world ocean. *Earth System Science Data*, *8*(2), 297–323. https://doi.org/10.5194/essd-8-297-2016

Pahnke, K., & Zahn, R. (2005). Southern Hemisphere Water Mass Conversion Linked with North Atlantic Climate Variability. *Science*, *307*(5716), 1741–1746. https://doi.org/10.1126/science.1102163

Ronge, T. A., Steph, S., Tiedemann, R., Prange, M., Merkel, U., Nürnberg, D., & Kuhn, G. (2015). Pushing the boundaries: Glacial/interglacial variability of intermediate and deep waters in the southwest Pacific over the last 350,000 years: Variability in SW-Pacific AAIW and UCDW. *Paleoceanography*, *30*(2), 23–38. https://doi.org/10.1002/2014PA002727

Rose, K. A., Sikes, E. L., Guilderson, T. P., Shane, P., Hill, T. M., Zahn, R., & Spero, H. J. (2010). Upper-ocean-to-atmosphere radiocarbon offsets imply fast deglacial carbon dioxide release. *Nature*, *466*(7310), 1093–1097. https://doi.org/10.1038/nature09288

Siani, G., Michel, E., De Pol-Holz, R., DeVries, T., Lamy, F., Carel, M., et al. (2013). Carbon isotope records reveal precise timing of enhanced Southern Ocean upwelling during the last deglaciation. *Nature Communications*, *4*(1). https://doi.org/10.1038/ncomms3758

Sikes, E. L., Elmore, A. C., Allen, K. A., Cook, M. S., & Guilderson, T. P. (2016). Glacial water mass structure and rapid $\delta^{18}O$ and $\delta^{13}C$ changes during the last glacial termination in the Southwest Pacific. *Earth and Planetary Science Letters*, *456*, 87–97. https://doi.org/10.1016/j.epsl.2016.09.043

Verdy, A., & Mazloff, M. R. (2017). A data assimilating model for estimating Southern Ocean biogeochemistry: SOUTHERN OCEAN BIOGEOCHEMISTRY ESTIMATE. *Journal of Geophysical Research: Oceans*, *122*(9), 6968–6988. https://doi.org/10.1002/2016JC012650